

Article

Morphological Analysis of a Nearshore Nourishment along the Atlantic Coast of New Jersey, USA

Sean P. McGill ^{1,*}, Brian D. Harris ¹, Brian C. McFall ¹ , Douglas R. Krafft ¹ , Rachel L. Bain ¹,
Nicholas R. Olsen ¹, Ian W. Conery ² and Monica A. Chasten ³

¹ Coastal and Hydraulics Laboratory, U.S. Army Engineer Research and Development Center, Vicksburg, MS 39180, USA

² Coastal and Hydraulics Laboratory-Field Research Facility, U.S. Army Engineer Research and Development Center, Duck, NC 27949, USA

³ U.S. Army Corps of Engineers, Philadelphia, PA 19107, USA

* Correspondence: sean.p.mcgill@usace.army.mil; Tel.: +1-601-634-2622

Abstract: Nearshore nourishment is a common coastal flood risk management technique that can be constructed beneficially by using dredged sediment from navigation channels. A nearshore nourishment project was completed during the summer of 2021 in Harvey Cedars, NJ, USA, with 67,500 m³ of dredged sediment from Barnegat Inlet placed along approximately 450 m of beach in a depth of 3–4 m. In situ instruments were installed to monitor hydrodynamic conditions before and after dredged material placement, and nine topographic and bathymetric surveys were conducted to monitor nearshore morphological response to the nourishment. Shoreline location was extracted from satellite imagery using CoastSat software to compare historical trends to the shoreline response after construction. Seven months after construction, 40% of the nearshore nourishment was transported from the initial footprint and the centroid of the nourishment migrated towards shore and alongshore (north). The sheltering capacity of the nearshore berm appears to have captured an additional 58% of the placed volume from the longshore transport system and the beach width onshore of the placement increased by 10.9 m. Measured data, satellite imagery analysis, and rapid predictions all indicate that the nearshore nourishment at Harvey Cedars had a positive impact on the adjacent beach.

Keywords: nearshore nourishment; sediment transport; shoreline extraction; shoreface nourishment



Citation: McGill, S.P.; Harris, B.D.; McFall, B.C.; Krafft, D.R.; Bain, R.L.; Olsen, N.R.; Conery, I.W.; Chasten, M.A. Morphological Analysis of a Nearshore Nourishment along the Atlantic Coast of New Jersey, USA. *J. Mar. Sci. Eng.* **2022**, *10*, 1622. <https://doi.org/10.3390/jmse10111622>

Academic Editor: Carlos Daniel Borges Coelho

Received: 8 October 2022

Accepted: 29 October 2022

Published: 2 November 2022

Publisher's Note: MDPI stays neutral with regard to jurisdictional claims in published maps and institutional affiliations.



Copyright: © 2022 by the authors. Licensee MDPI, Basel, Switzerland. This article is an open access article distributed under the terms and conditions of the Creative Commons Attribution (CC BY) license (<https://creativecommons.org/licenses/by/4.0/>).

1. Introduction

Nearshore nourishments are a common flood risk management technique used extensively around the world [1–6]. In the United States (US), nearshore nourishment projects are a common technique to beneficially use dredged sediment from navigation channels. From 2015 to 2020, the US Army Corps of Engineers (USACE) placed 28 Mm³ in nearshore littoral systems [7], which allows natural forces to redistribute the material and nourish the broader beach profile [8,9]. The primary objective of these nearshore beneficial use projects is to retain the sediment in the littoral system. Nearshore nourishment can beneficially use dredged sediment that is not suitable for a direct beach placement because the fine material is naturally winnowed from the placement by wave action [10,11]. Additional flood risk management benefits include nourishing the beach profile, breaking waves farther offshore [12], and extending the life of co-located subaerial beach nourishments [13].

Subaerial beach nourishment has been the leading form of coastal protection in the US for the last four decades [14] and commonly uses sediment from offshore sources. Direct subaerial nourishment is more expensive than nearshore nourishment [8], and sheltering the subaerial nourishment from erosive storm conditions using a co-located nearshore nourishment may have significant financial benefit. Consequently, some nearshore nourishments are placed in concentrated footprints as nearshore berms, which may have the capacity to break waves farther offshore and reduce their erosive potential [12,15]. This

potential to dissipate wave energy farther offshore has inspired research into co-located nearshore nourishments and subaerial beach nourishments [16].

Prior research suggests that the morphologic change around shallow nearshore nourishments results from two processes: (1) capturing alongshore sediment transport in the lee of the berm as waves break farther offshore, and (2) onshore transport driven by shoaling waves [17]. Both processes manifest as erosion in the placement footprint and accretion on the lee side of the placement. Placement monitoring via topographic and bathymetric surveys without direct sediment transport measurements can make it difficult to distinguish between these two nearshore processes in dynamic coastal environments. In one example where transport direction could be resolved (the nearshore nourishment tracer study in the controlled environment of the large-scale sediment transport facility [18]), the measurements suggested that alongshore transport can dominate the removal of material from the placement footprint in some settings [19]. In the field, nearshore nourishments are generally observed to migrate onshore, with a smaller number of placements remaining stable [20–24].

Although the nearshore placement of dredged sediment is common practice, the critical questions of how often the sediment will be mobilized, where the sediment will go, and how the shoreline will respond are often site-specific and remain poorly understood [22,24]. Nearshore nourishments have been studied with numerical modeling [25–27], physical modeling [28,29], and field measurements [10,14,22,30–32]. Although each method has its strengths and weaknesses, field monitoring is ideal in locations where projects are likely to be repeated because it allows for adaptive management of the project and improved outcomes of subsequent placements [33,34]. Monitoring nearshore nourishment projects commonly involves topographic and bathymetric surveys [35], hydrodynamic measurements [9,36], and shoreline response analysis from aerial imagery [37].

In the summer of 2021, sediment was dredged by the USACE Philadelphia District from the Barnegat Inlet federal navigation channel and used beneficially to construct a nearshore berm on the historically erosive beach at Harvey Cedars, NJ, USA [38,39]. To improve the understanding of the morphological evolution of nearshore nourishments and the adjacent beach response, this nearshore nourishment project was extensively monitored using a combination of in situ sensors and a series of topographic and bathymetric surveys. Satellite observations in conjunction with a trained machine learning algorithm were also utilized to track shore position at a higher temporal resolution and larger spatial extent than offered by traditional methodologies [40]. Knowledge gained from this monitoring will support future projects and advance the practice of nearshore nourishment.

2. Materials and Methods

2.1. Study Site

Harvey Cedars is a borough in Ocean County, NJ, USA, located along the barrier island of Long Beach Island approximately 110 km south of New York City, NY, USA (Figure 1a,b). Harvey Cedars has approximately 3 km of beach along the Atlantic Ocean. Wave Information Studies (WIS) hindcasts between 1976 and 1995 found Harvey Cedars had an average 0.9 m wave height and 6.4 s period from the southeast with most wave periods ranging from 5.0 to 9.0 s [41]. The site has a semi-diurnal tide range of 1.3 m [42]. A maximum wave height of 8.33 m and a 2% wave height of 3.22 m were recorded at the National Oceanic and Atmosphere Administration (NOAA) Station 44091 between 2015 and 2022 offshore of the project site. Harvey Cedars was selected to receive a nearshore nourishment because of an erosional hotspot identified along a stretch of shoreline within the Federal Coastal Storm Risk Management (CSRM) Project, which stretches for 26 km along Long Beach Island, NJ, USA. The Harvey Cedars beachfill portion of CSRM was originally completed in July 2010 [38] using 2.4 Mm³ of sediment, expanding the beach and burying a groin field (Figure 1c). Since that time, an emergency beachfill in 2013 used 1.2 Mm³ of sediment to repair damages to the beach and dune system after Hurricane Sandy, and 0.9 Mm³ of sediment was used for a periodic nourishment in 2018.

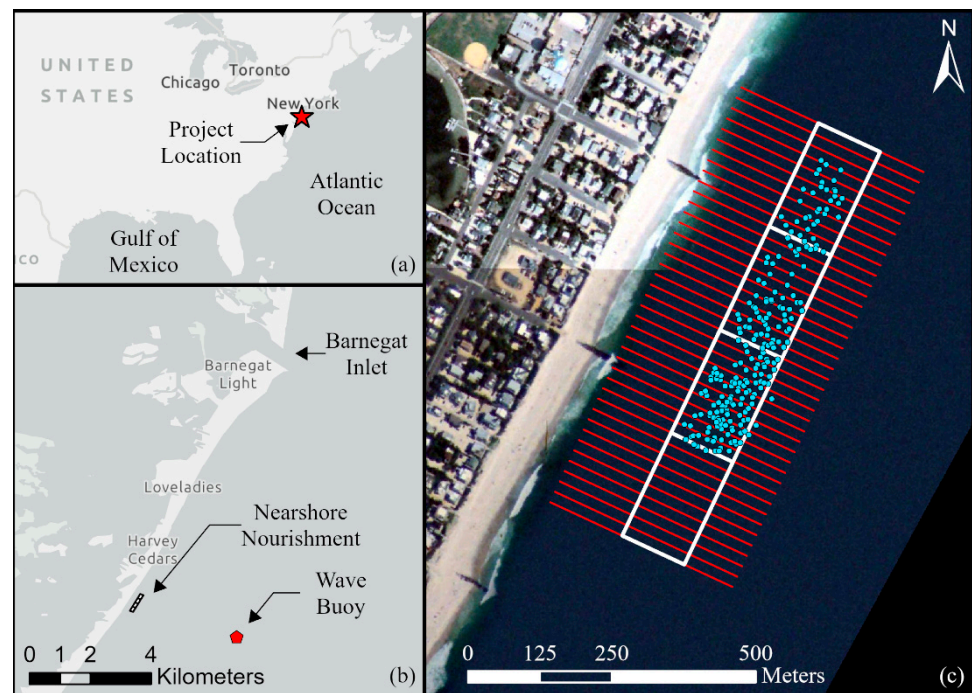


Figure 1. (a) Project location, (b) Barnegat Inlet and Harvey Cedars, and (c) the design extent of the nourishment divided into four 150 m wide sections. Vessel heading lines spaced at 15 m shown in red and blue circles denote drop locations. (c) contains Landsat/Copernicus imagery from Google Earth.

In July and August 2021, the USACE Philadelphia District placed 67,500 m³ of dredged sediment in the nearshore of Harvey Cedars, NJ, USA, approximately 100 m from shore ([38,39]; see Figure 1c). The sediment was dredged from Barnegat Inlet, a federal navigation channel located approximately 10 km north of the placement site. The dredged sediment consisted of sandy material with a median grain size of 0.42 mm. Barnegat Inlet was one of the 10 beneficial use pilot projects that the Water Resource and Development Act (WRDA) Section 1122 program established across the nation and was carried out by USACE Philadelphia District in partnership with the NJ Department of Environmental Protection. The nearshore nourishment was constructed using the USACE's split hull hopper dredge *Murden* to remove sediment from shoals in the channel and transport dredged material south to Harvey Cedars. The *Murden* has a hull capacity of 380 m³ and could complete a trip, which includes dredge time and travel to and from the site, in approximately 3 h. The design of the nearshore berm consisted of four 150 m wide shore-parallel boxes with their landward side at the −2.75 m NAVD88 contour line (Figure 1c). Vessel heading lines were spaced every 15 m, and the dredge was instructed to “nose in” along the placement line and then split the hopper to place the sediment as shallow as possible given the tide. The average placement depth was 3–4 m. The dredge began construction at the north end of the southernmost box and placed multiple loads per line before progressing north. Approximately halfway through construction, the dredge reduced the number of drops per line to develop a longer berm [39], resulting in the northern half of the berm being less prominent when compared to the southern end.

2.2. In Situ Instruments

A variety of hydrodynamic data were collected at 3 locations in the area around the nearshore nourishment with 3 distinct water depths to measure the forcing of the morphological response to nearshore nourishment. From 23 June 2021 to 10 May 2022, an RBR Virtuoso pressure sensor was deployed 630 m north of the nearshore nourishment in 1.5 m of water. Another pressure sensor was deployed landward of the nearshore nourishment at the same time in a similar water depth, but the data could not be recovered. Pressure

measurements from the surviving RBR sensor were converted to bulk wave statistics to quantify nearshore wave characteristics in the immediate vicinity of the nearshore nourishment. The instrument was installed in close proximity to buried groins that periodically became exposed during the project monitoring and may have influenced the nearshore wave characteristics. The measurements from the RBR sensor are described in greater detail in the Results section. From 7 December 2021 to 15 April 2022, an ADCP measured water level and vertical velocity profiles in 8 m of water on the seaward edge of the nearshore nourishment at 4 Hz for 34 min each hour. These data were collected for future numerical model validation at the site. A Sofar Spotter buoy collected hourly wave spectra approximately 3 km offshore of the site in 15.2 m of water (Figure 1b). The buoy collected wave data between 1 July 2021 and 17 December 2021, after which it became unmoored. After 17 December 2021, wave data from NOAA Station 44091 were substituted to understand wave conditions offshore of the nourishment and calculate sediment transport rates. Information about sensor deployments is summarized in Table 1.

Table 1. Sensor deployment information.

Sensor	Location	Approximate Depth	Timing
RBR Virtuoso (Pressure)	630 m North of the nourishment	1.5 m	23 June 2021 to 10 May 2022
Nortek Signature 1000 (ADCP)	Seaward of the nourishment	8.0 m	7 December 2021 to 15 April 2022
Sofar Spotter buoy (Spectral wave info)	3 km offshore of nourishment	15.2 m	1 July 2021 to 17 December 2021

2.3. Site Evaluation for Nearshore Nourishment

Several commonly applied techniques have been previously developed to rapidly assess potential nearshore nourishment sites [24]. These include approximating the depth of closure [43–46], frequency sediment placed in the nearshore will be mobilized [47], the cross-shore transport direction [48], and comparing the potential site to historical projects [20]. All of these techniques can be applied in the interactive Sediment Mobility Tool web application [49] and the methods are detailed here.

The depth of closure is the depth beyond which repeated beach profiles compiled over time converge [50] or the depth along a beach profile where there is not significant sediment transport from nearshore processes [51]. Hallermeier [43,44] further defined an inner depth of closure and outer depth of closure. The outer depth of closure (h_i) is the depth at which waves cause minimal sediment transport and is calculated as

$$h_i = (\overline{H_s} - \sigma_s) \overline{T_s} \left(\frac{g}{5000 d_{50}} \right)^{0.5} \tag{1}$$

where $\overline{H_s}$ is the mean annual significant wave height, σ_s is the significant wave height standard deviation, $\overline{T_s}$ is the average period associated with $\overline{H_s}$, g is the gravitational constant, and d_{50} is the median sediment grain size. The inner depth of closure (h_l) is the seaward boundary for the littoral zone where the bed experiences increased significant stresses and sediment transport from wave near breaking and nearshore circulation. The inner depth of closure is the appropriate limit for the shoreline response and beach nourishment projects [52]. The equation to calculate the inner depth of closure (h_l) is given by Hallermeier [43] as

$$h_l = 2.28H_e - 68.5 \left(\frac{H_e^2}{gT_e^2} \right) \tag{2}$$

where H_e is the effective wave height, or the wave conditions exceeded only 12 h per year (largest 0.137% waves in a year), and T_e is the wave period associated with H_e . Birke-meier [45] evaluated Equation (2) using high fidelity bathymetric profiles from the USACE

Field Research Facility in Duck, NC, USA from June 1981 to December 1982, and found the more appropriate coefficients for the equation for this site to be

$$h_l = 1.75H_e - 57.9 \left(\frac{H_e^2}{gT_e^2} \right) \tag{3}$$

Hands and Allison [20] compared the Hallermeier inner (Equation (2)) and outer (Equation (1)) depth of closure values at 11 historical nearshore berm sites to analyze the relationship between the equations and whether the placements were stable or active. Stable berms maintained most of the placed volume for years, whereas the active berms dispersed within months. All the berms built shallower than the inner depth of closure were active, and the one nearshore berm built deeper than the outer depth of closure was stable. This analysis was expanded by McFall et al. [24] to include a total of 20 historical projects, and similar trends emerged.

Another technique to estimate how active a nearshore nourishment will be at a site is to calculate how often placed sediment is expected to be mobilized. This is calculated by the Sediment Mobility Tool in two different ways [47]. One method uses bed shear stress and linear wave theory using the technique described by Soulsby [53]. The critical bed shear stress to initiate sediment mobility is calculated as

$$\tau_{cr} = \theta_{cr} g (\rho_s - \rho) d_{50} \tag{4}$$

where θ_{cr} is the Shields parameter, ρ_s is the sediment density, and ρ is the water density. The maximum bed shear stress is calculated using the bed shear stress induced by the waves and current as

$$\tau_m = \tau_c \left[1 + 1.2 \left(\frac{\tau_w}{\tau_c + \tau_w} \right)^{3.2} \right] \tag{5}$$

and

$$\tau_{max} = \left[(\tau_m + \tau_w \cos\phi)^2 + (\tau_w \sin\phi)^2 \right]^{1/2} \tag{6}$$

where τ_m is the mean bed shear stress, τ_c is the current induced bed shear stress, τ_w is the wave induced bed shear stress, and ϕ is the angle between the wave and current direction. To quantify the average normalized difference of the maximum shear stress and the critical threshold, the mean mobility score (M) is calculated as

$$M = \left(\frac{\tau_{max} - \tau_{cr}}{\tau_{cr}} \right) \tag{7}$$

The second method to calculate the sediment mobility uses the near-bottom velocity and nonlinear stream function wave theory using a procedure described by Ahrens and Hands [21]. The critical near-bottom velocity (u_{cr}) for sediment with grain size diameter less than 2 mm is calculated as

$$u_{cr} = \sqrt{8g\gamma d_{50}} \tag{8}$$

where $\gamma = (\rho_s - \rho)/\rho$. The maximum wave induced near-bottom velocity for the wave crest and wave trough are calculated as

$$u_{maxcrest} = \left(\frac{H}{T} \right) \left(\frac{h}{L_0} \right)^{-0.579} \exp \left[0.289 - 0.491 \left(\frac{H}{h} \right) - 2.97 \left(\frac{h}{L_0} \right) \right] \tag{9}$$

and

$$u_{maxtrough} = - \left(\frac{H}{T} \right) \exp \left[1.966 - 6.70 \left(\frac{h}{L_0} \right) - 1.73 \left(\frac{H}{h} \right) + 5.58 \left(\frac{H}{L_0} \right) \right] \tag{10}$$

where H is the wave height at the placement site, T is the wave period, h is the water depth, and L_0 is the offshore wavelength given by $L_0 = (g T^2) / 2 \pi$. The maximum near-bottom

velocity was taken as $u_{max} = \max(|u_{maxcrest}|, |u_{maxtrough}|)$. The mean mobility score for this method is calculated as

$$M_u = \left(\frac{u_{max} - u_{cr}}{u_{cr}} \right) \tag{11}$$

For the site evaluation at this project, the Sediment Mobility Tool was applied using wave characteristics from the offshore WIS Station 63137 transformed to the nearshore depth of 4 m using Snell’s Law and conservation of energy flux. The sediment mobility analysis was applied to hourly hindcasts for 10 years (1 January 1990–31 December 1999).

2.4. Surveys

Nine topographic and bathymetric surveys were performed throughout the duration of this project. These surveys consisted of 26 lines of single-beam and RTK-GPS transects at 75 m spacing, combined with periodic multi-beam surveys in the immediate area surrounding the nearshore placement. Table 2 shows a summary of completed surveys and methods for the project. The location of the MHHW contour at 0.61 m NAVD88 was extracted at each of the transects for each survey. The survey data were then combined to create Digital Elevation Models (DEMs) for site analysis. A change map based on pre- and post-placement elevations was used to create a mask for the initial placement’s extent. Additional change maps between successive survey dates were created, and the berm mask was used to extract the placement area for sediment centroid calculations and volume change analysis.

Table 2. Survey information.

Survey Type	Date	Period	Notes
Single-Beam	13 May 2021	Pre-Nourishment	-
Multi-Beam	22 July 2021	During Construction	-
Multi-Beam	28 July 2021	During Construction	-
Multi-Beam	9 August 2021	During Construction	-
Single- and Multi-Beam	25 August 2021	Post Placement	6 days post construction
Single- and Multi-Beam	13 October 2021	Post Placement	55 days post construction
Single- and Multi-Beam	9 December 2021	Post Placement	112 days post construction
Single-Beam	22 March 2022	Post Placement	215 days post construction
Single-Beam	17 June 2022	Post Placement	302 days post construction

2.5. Deflation Code

A method for generating order-of-magnitude estimates of sediment loss from a nearshore placement site was previously developed by Bain et al. [54]. Time series measurements of wave height, period, and direction are used to estimate longshore and cross-shore transport rates. The longshore transport (Q_y) is calculated using the equation by Shaeri et al. [55] as

$$\frac{Q_y T_p}{H_b^3} = \frac{3 \times 10^{-4}}{(1 - a)} \frac{\rho_w}{\rho_s - \rho_w} \left(\frac{H_b}{L_0} \right)^{-0.9} \left(\frac{H_b}{d_{50}} \right)^{0.2} \sin^{0.5}(2\theta_b) \tag{12}$$

where T_p is the peak wave period, H_b is the breaking wave height, and a is the porosity that is set to 0.4. The coefficient in Equation (12) was calibrated using 47 longshore transport datasets from sites around the world [55]. The cross-shore transport (Q_x) is calculated per unit width using a modified method from Dronkers [56] as

$$Q_x = \alpha [-\lambda m \langle |u_w|^3 \rangle + \langle |u_w|^2 u_w \rangle (1 - k)] \cos \theta_{crest} \tag{13}$$

where α and λ are empirical coefficients, m is the bed slope, u_w is the near-bottom horizontal velocity, k is the critical velocity scaling term and is given as $k = \min[u_{cr}/u_w^{max}, 1]$, and θ_{crest} is the wave angle over the crest of the nearshore berm. Angular brackets $\langle \rangle$ indicate averaging over a wave period. The negative term in Equation (13) represents the gravity-driven offshore transport, whereas the positive term represents the wave-driven onshore transport. Hudson et al. [57] used a series of placements at the Columbia River mouth to optimize the empirical parameters in Equation (13) as $\alpha = 3 \times 10^{-5}$ and $\lambda = 1.7$, which are retained as constants in the present study. Superimposing the longshore and cross-shore sediment transport rates predicted by Equations (12) and (13) and integrating over a specified time period yields an estimate of the total volume of sediment removed from the original placement footprint. The validation in Bain et al. [54] achieved acceptable order-of-magnitude deflation rate predictions at 11 historical nearshore placements along the Atlantic, Pacific, and Gulf Coasts of the United States with the same empirical parameters as Hudson et al. [57] and Shaeri et al. [55].

To test this methodology for the Harvey Cedars placement, the sediment transport algorithm was forced using Spotter Buoy wave measurements from 8 July 2021 until 9 December 2021. Wave data from NOAA Station 44091 (32 km northeast of the placement site at 25.6 m depth) were used to force the model from 9 December 2021 until 22 March 2022 due to the unmooring of the Spotter Buoy in mid-December. Conditions were not modeled following the March survey due to missing data from NOAA Station 44091 beginning in April until June. For both sources of wave data, the offshore significant wave height was transformed to height across the nearshore profile based on conservation of energy flux (e.g., Komar [50]), and the offshore wave direction was transformed to direction at breaking using Snell’s Law. Following the approach of Bain et al. [54], the placement’s geometric parameters were treated as time-invariant and were based on the shape and position of the sediment mound during the first post-placement survey on 25 August 2021, as summarized in Table 3.

Table 3. Site parameters used to generate order-of-magnitude predictions of the sediment volume loss from the Harvey Cedars placement site.

Parameter	Value (Treated as Time-Invariant)
Shore angle	210°
Landward boundary of initial placement footprint	168 m
Cross-shore distance to initial placement crest	198 m
Seaward boundary of initial placement footprint	290 m
Water depth at landward placement boundary	3.0 m
Water depth at initial placement crest	2.5 m
Water depth at seaward placement boundary	7.9 m
Shore-parallel length of placement	427 m
Representative beach slope	0.03
d_{50} of placed sediment	0.42 mm
Water density	1025 kg/m ³
Sediment density	2650 kg/m ³
Sediment porosity	0.4

2.6. Satellite Analysis

The open-source CoastSat tool [40] was used to track shoreline position in the vicinity of the placement from January 2001 to May 2022 using satellite imagery collected from the Landsat 5 and Landsat 8 missions. Landsat 5 collected imagery from 1984 to 2013, whereas Landsat 8 began in 2013 and is still ongoing. Both missions have revisit periods of

16 days, and 30 m pixel resolution across Red, Green, Blue, Near Infrared, and Short-wave Infrared 1 bands. This software toolkit uses a trained multi-layer perceptron algorithm to classify pixels in multispectral imagery as land or water and calculates the normalized difference water index (NDWI) from observations downloaded from Google Earth Engine’s public repository [40]. Otsu’s thresholding algorithm is applied to the pairs of categorized and NDWI rasters [58]. These thresholds attempt to depict the land-water interface at the time of observation. Each pansharpended image, overlaid with corresponding shoreline detection, has been checked to ensure that only high-quality detections are used in analysis. The resulting collection of quality-checked shorelines can be used to track the shoreline position through time. Satellite-derived shorelines were filtered using a 45-day moving average with a 15-day step to capture the rapid shoreline response to the nourishment.

3. Results

3.1. Wave Analysis

Wave conditions during the monitoring period are shown in Figure 2. At the Spotter buoy (3 km offshore of the placement site in 15.2 m of water), the mean and median significant wave heights were $H_s = 0.91$ m and $H_s = 0.82$ m, respectively, with a maximum of $H_s = 3.12$ m (Figure 2a). The mean peak period was $T_p = 8.3$ s, and the median was $T_p = 7.9$ s. The most frequent offshore wave direction was between 90° and 120° relative to north (between 0° and 30° relative to shore-normal); however, waves between 120° and 180° relative to north (between -60° and 0° relative to shore-normal) were also common (Figure 2b). It should be noted that the Spotter buoy became unmoored after 17 December 2021, so the wave conditions in Figure 2a,b do not include data from winter storm waves.

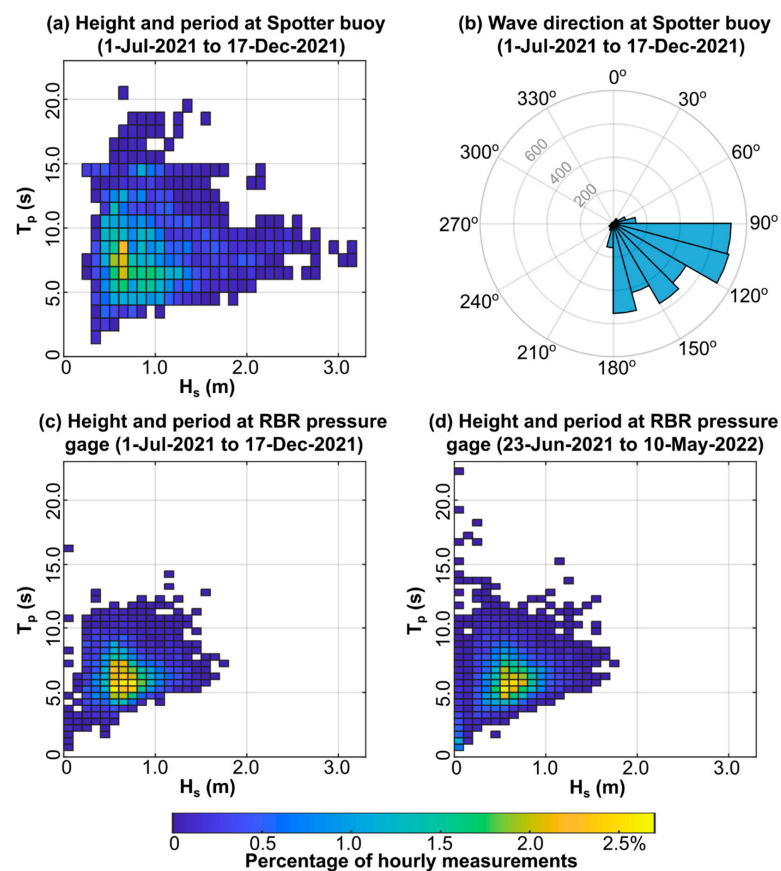


Figure 2. Distribution of offshore and nearshore wave conditions. (a) Wave height and period at the Spotter buoy, 3 km offshore of the placement site. (b) Wave direction at the Spotter buoy. The concentric circles indicate the number of hourly events, and all angles are relative to north. (c) Wave height and period at the RBR pressure gauge for the same time period shown in subplot (a). (d) Wave height and period at the RBR pressure gauge for the entire monitoring duration.

Nearshore wave measurements from the RBR pressure gauge (630 m north of the nourishment, in approximately 1.5 m of water) indicate that smaller-amplitude, higher-frequency waves are most common near the placement site. For the same time period recorded by the Spotter buoy, the mean, median, and maximum nearshore significant wave heights were $H_s = 0.69$ m, $H_s = 0.65$ m, and $H_s = 1.73$ m, respectively (Figure 2c). The mean peak period was $T_p = 6.4$ s with a median of $T_p = 6.2$ s. Over the full monitoring duration (23 June 2021 to 10 May 2022; Figure 2d), these values change to a mean $H_s = 0.60$ m, median $H_s = 0.59$ m, mean $T_p = 6.1$ s, and median $T_p = 6.0$ s.

3.2. Site Evaluation for Nearshore Nourishment

The Hallermeier inner and outer depths of closure were calculated to be 8.8 m and 14.0 m, respectively. The Birkemeier inner depth of closure was calculated as 6.7 m. The project placement depth is plotted in relation to the Hallermeier depth of closure values in Figure 3 for comparison with 20 historical nearshore nourishment projects. The placement depth was shallower than both the inner and outer depths of closure, indicating that this project is similar to highly active historical nearshore nourishment projects.

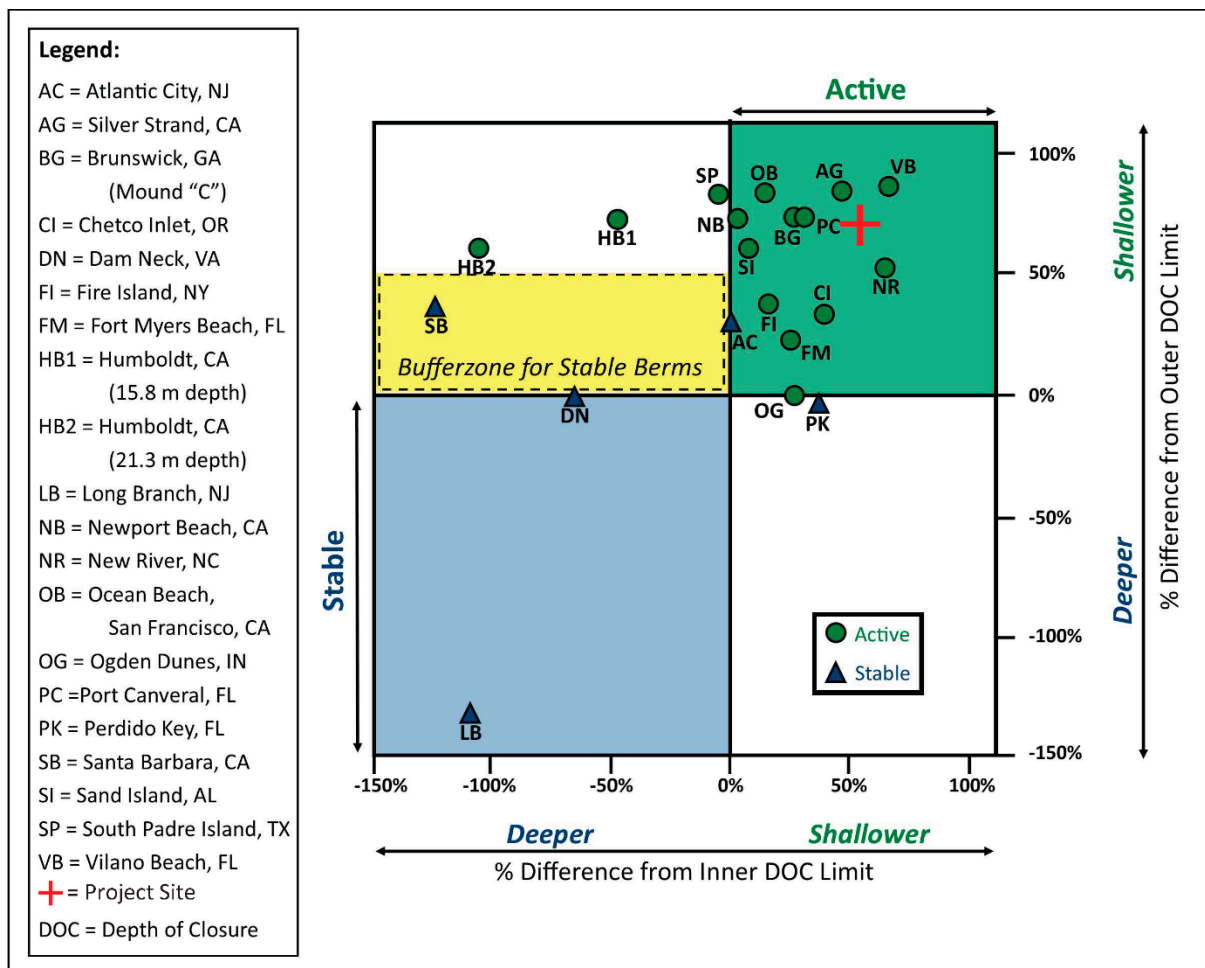


Figure 3. Relationship of the nearshore nourishment site to the Hallermeier depth of closure equations and compared to historical projects (adapted from McFall et al. [24] and Hands and Allison [20]).

The frequency of sediment mobility was also calculated. The median grain size of 0.42 mm is estimated to be mobilized by 91% of the waves using linear wave theory and 95% of the waves using stream function theory, as shown in the histograms in Figure 4. The mobility scores greater than 2 indicate a very active site. Mobility scores less than 1 tend to be stable projects [23]. These rapid site evaluation techniques indicate the project site

will be very active, nourishing the beach profile. The placed sediment is predicted to be mobilized frequently because the placement was constructed at a relative depth and wave climate similar to historically active projects.

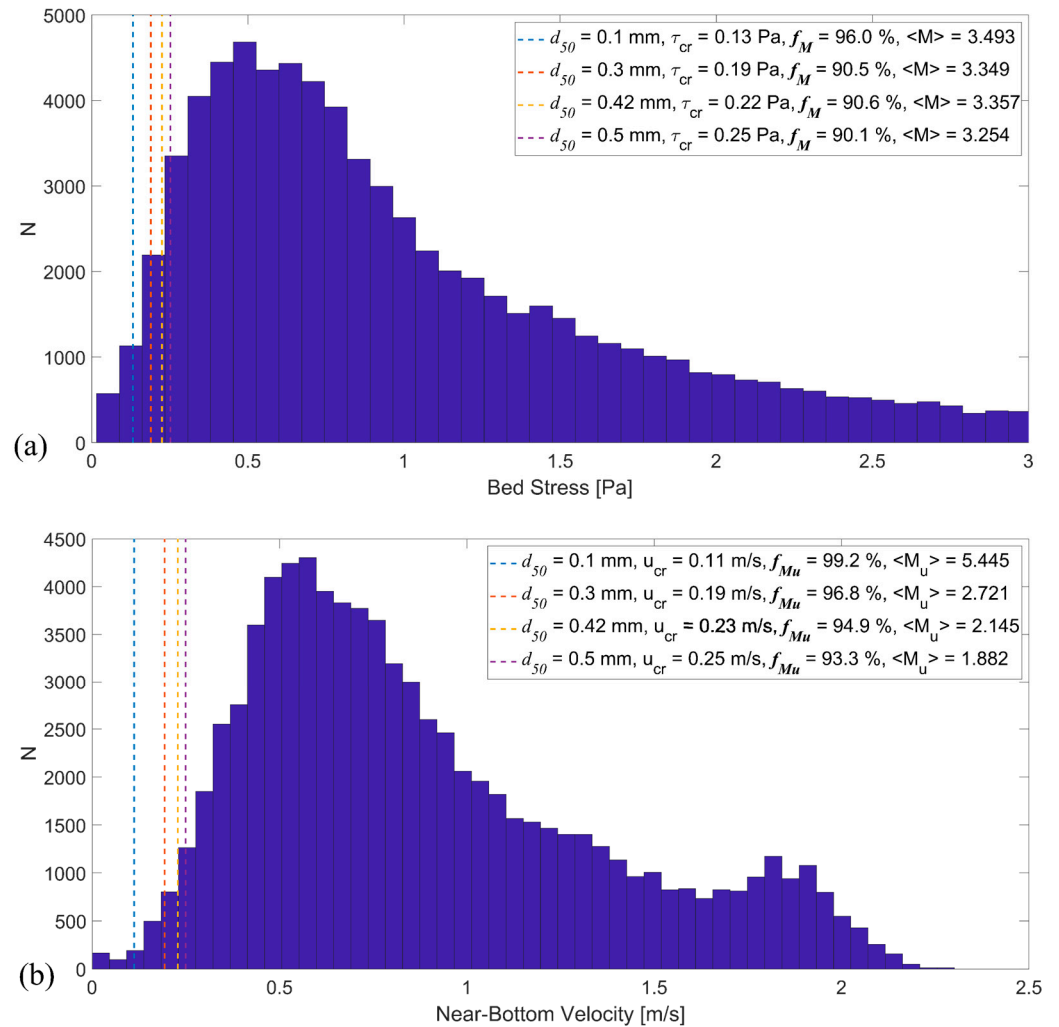


Figure 4. Histograms of the (a) bed shear stress and (b) near-bottom velocity calculated for the nearshore placement. The vertical dashed lines are the thresholds to initiate sediment mobility for the respective grain sizes.

3.3. Surveys

A total of 67,500 m³ of sediment was placed in the nearshore during the construction of the nearshore berm, and 26,700 m³ of sediment was transported away from the placement between the completion of construction in August 2021 and March 2022. Figure 5 shows the change in nearshore morphology during and after the construction of the berm. The centroid of the berm migrated toward the north throughout the surveys, with the exception of the June 2022 survey due to two Nor'easters that occurred in April and May. As seen in Figure 5b, sediment accretion occurred at the shoreline directly landward of the berm, as well as in the nearshore surrounding the initial placement. Minor avalanching of sediment on the seaward slope of the berm also occurred. Analysis of the three cross-shore transects drawn in Figure 5a shows the change in beach profiles throughout the surveys (Figure 6). Beach profile change was the most variable along the site transect post construction, with nearshore elevations increasing from the placement (Figure 6b). Between post-construction and the 22 March 2022 survey, the beach width above the MHHW line increased by 10.9 m before receding in the June 2022 survey.

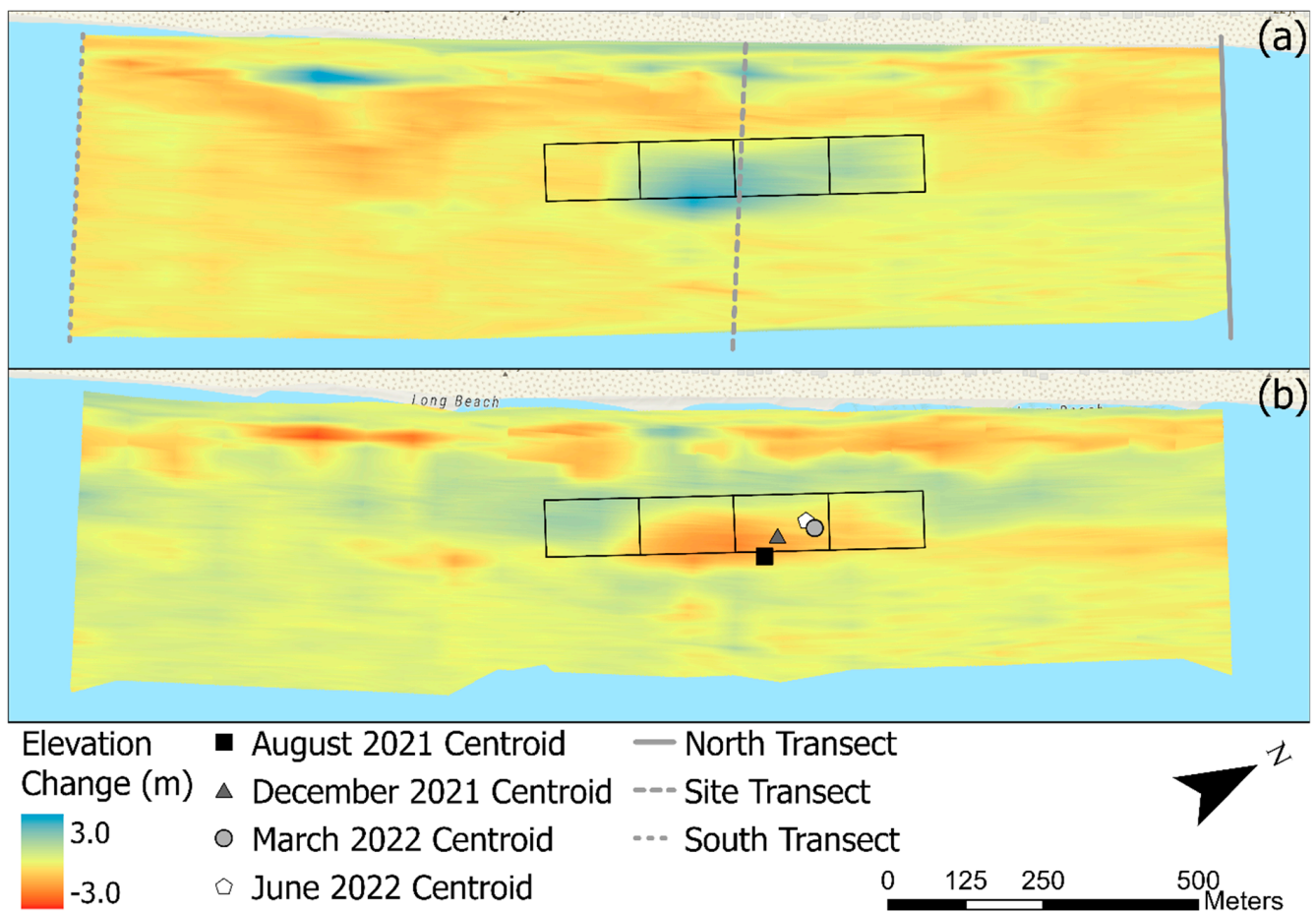


Figure 5. Change maps between pre- and post construction (a) and post construction and June 2022 survey (b). Within the placement area, the centroid of sediment was found and labeled for the surveys in August 2021, December 2021, March 2022, and June 2022.

3.4. Deflation Results

A time series of the predicted volumetric sediment transport rate at the placement site appears in Figure 7. Sediment loss within the placement footprint due to longshore transport remains near zero except during large wave events, when the breaking position is farther offshore (Figure 7a). Cross-shore removal of sediment from the placement site is predicted to occur more frequently (Figure 7b) but with a smaller maximum magnitude than calculated for the large longshore transport events that occurred in January and February 2022. Due to the shape of a wave under stream function wave theory (Equations (9) and (10)), the net transport over a single wave period tends to be onshore in shallow water. Instances of offshore transport predictions were considered minimal as they were 5 orders of magnitude smaller than onshore transport and were rounded to zero for our analysis. Time-integrating the volume loss rates in Figure 7 predicts that approximately 34,000 m³ of sediment was removed from the placement footprint via longshore transport between 25 August 2021 and 22 March 2022, whereas approximately 31,400 m³ was removed via cross-shore transport over the same time period for a total predicted volume loss of 65,400 m³ (Table 4), i.e., almost the entire placed volume of sediment. The actual volume loss from the original footprint over the same timespan was 26,700 m³, or a predictive error of 145% of the bulk volume removal rate.

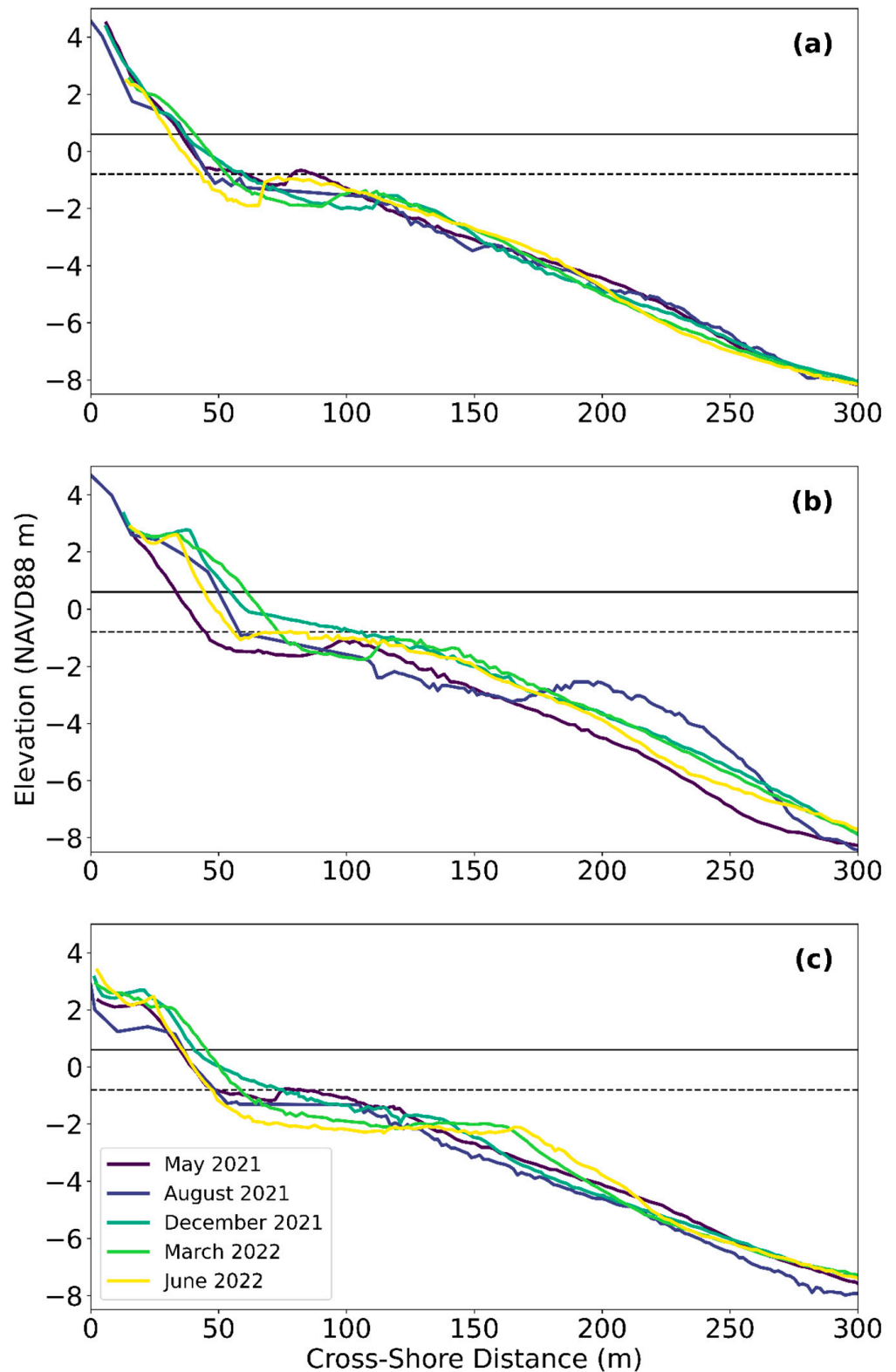


Figure 6. Beach profiles along the most northern transect (a), a transect within the placement area (b), and a transect south of the placement (c). MHHW (black solid line) is 0.61 m, and MLLW (black dashed line) is -0.79 m. The nearshore berm is seen in the August 2021 survey in (b) between 165 and 285 m.

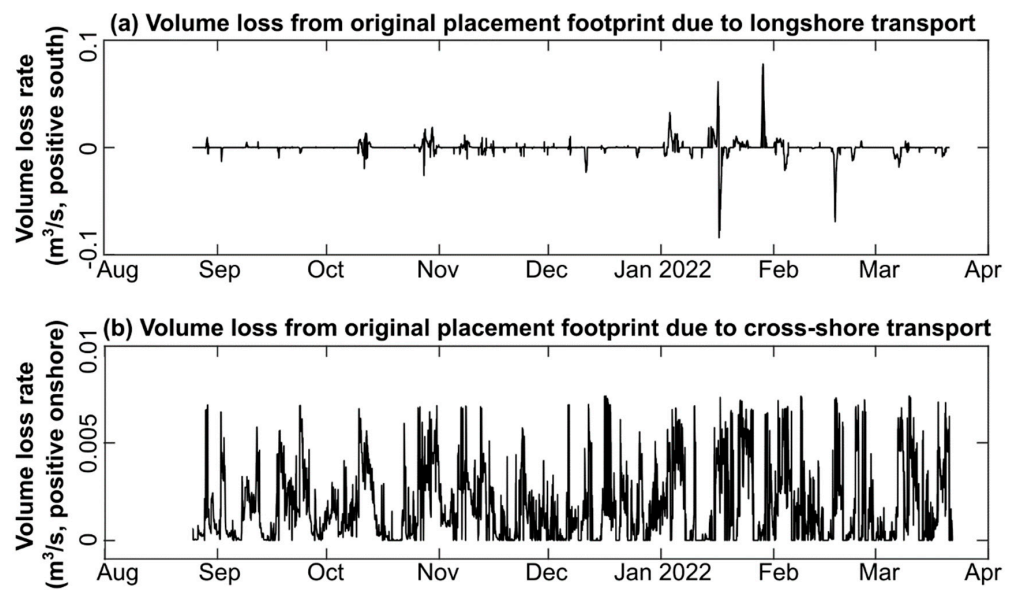


Figure 7. Time series of predicted volumetric sediment transport away from the original placement footprint based on the algorithm of Bain et al. [54]. In subplot (a), transport is directed alongshore towards the south when positive and alongshore towards the north when negative. In subplot (b), transport is directed onshore when positive and offshore when negative. Note that the cross-shore transport rate is for the entire shore-parallel length of the placement footprint (i.e., not unit width).

Table 4. Predicted volume of sediment lost from the original placement footprint between consecutive bathymetric surveys and the full monitoring duration. Values are rounded to the nearest hundred.

t_{start}	t_{end}	Predicted Volume Loss from Original Placement Footprint between t_{start} and t_{end} (m^3) *				
		Southward	Northward	Onshore	Offshore	Sum of All Directions
25 August 2021	13 October 2021	1800	1200	7100	0	10,100
13 October 2021	9 December 2021	2900	1800	7500	0	12,200
9 December 2021	22 March 2022	12,000	14,300	16,800	0	43,100
25 August 2021	22 March 2022	16,700	17,300	31,400	0	65,400

* From 25 August 2021 to 9 December 2021, the sediment transport model is forced using wave data from the Spotter Buoy. After 9 December 2021, the model is forced using wave data from NOAA Station 44091. Regardless of the data source, wave direction and height were transformed to nearshore values using Snell’s Law and conservation of energy flux.

Bain et al. [54] validated their results for total (longshore + cross-shore) sediment removal from 11 historical placement sites but had insufficient survey data to evaluate whether the *direction* of predicted transport was accurate. To further evaluate the algorithm’s ability to accurately predict relative proportions of longshore versus cross-shore sediment removal from a placement site, a grid surrounding the placement area was created and used to divide the bathymetric survey data (Figure 8). The change in sediment volume within each quadrant was then calculated for each pair of consecutive surveys. Between placement and March 2022, 16,000 m^3 of sediment accreted directly onshore, 9900 m^3 of sediment accreted directly offshore, 3200 m^3 accreted north of the placement and 36,900 m^3 accreted to the south of the placement (Figure 8). The surrounding area gained 145% more sediment than the placement area lost, indicating sediment from the longshore transport was retained in the project area. The previously noted predicted deflation of the nearshore nourishment (65,400 m^3) is coincidentally similar to the total volume gained in the areas surrounding the nourishment area (65,700 m^3), but the volume gain accounts for processes not accounted for in the predicted deflation.

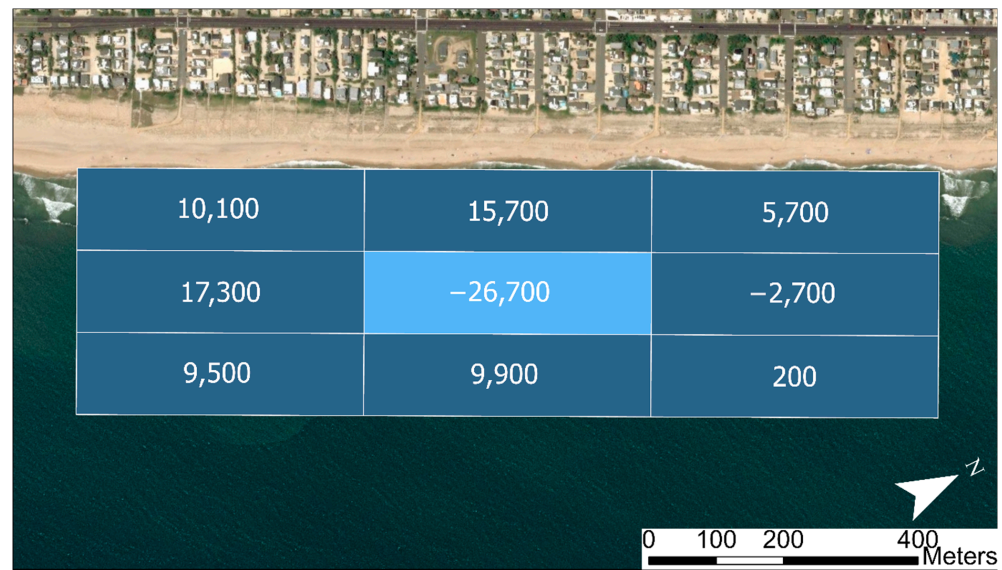


Figure 8. Sediment volume change grid between 25 August 2021 and 22 March 2022 surveys in m^3 . The initial placement area is in the center of the grid, indicated by lighter shading.

3.5. Shoreline Change

Shoreline change in the study area was investigated with a combination of satellite imagery and surveys. Satellite images were analyzed from 2000 onwards to investigate long-term shoreline position, showing two major trends separated by the first of four nourishment projects. From 2000 until 2010, beach width remained stable with some seasonal variability. Starting with the first major recent nourishment in 2010, beach width increased up to 120 m at the site transect (Figure 9b). After project construction, subaerial equilibration was accelerated by Hurricanes Irene (2011) and Sandy (2012), and the satellite data shows the beach returned to pre-project width after approximately 36 months following a shoreline retreat rate of -39.3 m/year (Figure 9b). Hurricane Sandy triggered an emergency nourishment which returned the beach to roughly the 2010 post-nourishment width. Following the most recent beachfill in 2018, the satellite-derived shoreline appears to be remaining stable south of the site, but retreated up to 50 m at the site and 62 m north before the 2021 nearshore nourishment (Figure 9b). Following the 2021 nearshore nourishment at Harvey Cedars, surveys between October 2021 and March 2022 show the nearby shoreline generally advanced, with erosion in the southern half of the placement footprint (Figure 9a). Elevation data indicates that the shoreline retreated over much of the surveyed area between March and June 2022, generally eroding past the recent accretion (Figure 9a). The universal erosion shown in the June shoreline was due to a Nor'easter impacting the study site from 7 May 2022 to 12 May 2022.

Shore position was derived from satellite imagery at 49 transects at and near the placement area from the year preceding the placement to present to investigate alongshore spatial patterns more thoroughly (Figure 10). These changes are unfiltered and relative to 3 October 2020 shore position. The alongshore area in the immediate vicinity of the placement falls between the two black lines overlaying the image. All change values were subtracted by the average values of all transects to isolate local variation from trends seen across the region. CoastSat analysis generally captures the shoreline advance that the survey data indicated across much of the placement area following project construction, with more accretion near the center of the placement area. Comparison of the shoreline from surveys to CoastSat-derived shoreline allows for error quantification at specific transects. The shoreline farther north was generally erosive in CoastSat analyses over the same time span, typically underestimating the shoreline change with an average error of 5.10 m. Satellite analysis south of the placement area indicates a mix of shoreline accretion and erosion in this timespan; that is, the shoreline is less accretionary relative to inside

the placement area. This was the most accurate of the three transects, with a 3.69 m underestimation error skewed by the October 2021 and June 2022 surveys. Alongshore patterns of satellite-derived shoreline change appear to indicate more accretion landward of the nearshore nourishment than in the surrounding area, although this section also has the greatest error, overestimating shoreline change by an average of 9.96 m when compared to elevation surveys.

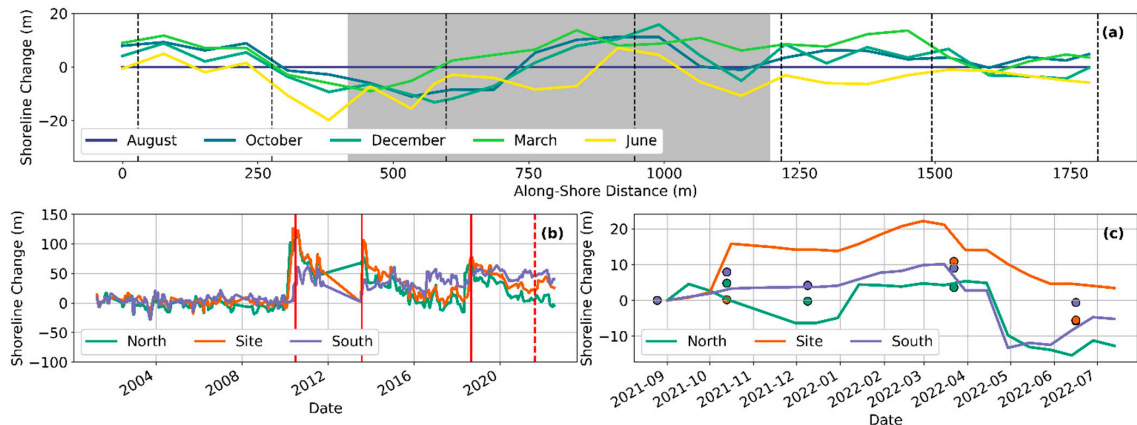


Figure 9. Change in mean shoreline extracted from the surveys (a), extracted shoreline from satellite imagery over the past 20 years (b), and comparing satellite extracted shoreline and survey extracted shoreline after construction (c). For the elevation surveys, shoreline change is relative to the post-construction August survey, groin locations are the dashed black lines, and the placement area is highlighted in grey. Previous subaerial beach nourishment projects are shown with solid red lines, with a dashed red line representing the 2021 nearshore nourishment (b), and DEM extracted shorelines are depicted as circles (c).

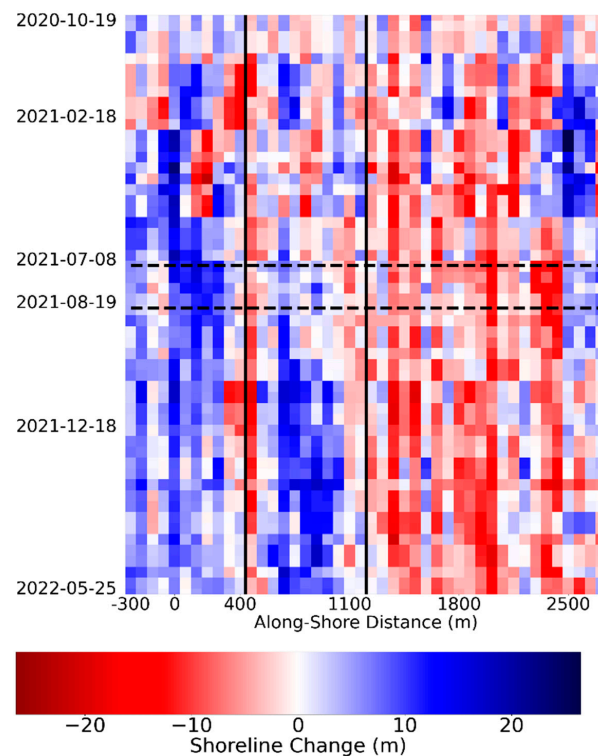


Figure 10. Change in raw shoreline extracted from the satellite imagery relative to the 3 October 2020 shoreline and normalized using the mean of all transects to remove tidal influences. The vertical solid lines show the along shore position of the nearshore nourishment, and the horizontal dashed lines frame the time of construction.

4. Discussion

The combination of collected data and analyses performed for the nearshore nourishment at Harvey Cedars can be compared to further describe the placement evolution and the effectiveness of predictive capabilities. Elevation survey data indicates that the nearshore berm deflated by 40% between 25 August 2021 and 22 March 2022. During this timespan, the nearshore berm appears to merge with the local sandbar system. Shoreline position from elevation surveys shows accretion along the northern half of the placement until the June 2022 survey. Shoreline retreat in the June 2022 survey could be related to the impacts of large Nor'easters in April and May. In addition to shoreline advance, a large volume of sediment had accreted south of and onshore of the initial placement footprint in the March 2022 survey. Centroid tracking at the nearshore berm indicates migration to the north in all but the June 2022 survey, implying that the accretion south of the placement was on the updrift side. Updrift and onshore accretion and downdrift erosion would generally match the Van Duin et al. [17] predicted sediment transport pattern of longshore trapping at nearshore berms. Although the nourishment footprint deflated $26,700 \text{ m}^3$, the survey area surrounding the nourishment gained $65,700 \text{ m}^3$, or an additional 145% more than was deflated, which is similar to the observed morphological response at Terschilling [59] at a much smaller scale ($67,500 \text{ m}^3$ of placed sediment vs. 2 Mm^3).

Shoreline advance is also visible in CoastSat analysis of satellite imagery, demonstrating the satellite extracted shoreline approach is capable of monitoring the evolution of coastal management practices such as nearshore nourishment. The nearshore berm at Harvey Cedars is the first to be investigated with CoastSat, enabling more frequent measurements at a higher alongshore resolution than is feasible with traditional survey methods. Satellite-derived shorelines show the most shoreline advance in the lee of the nearshore berm, which is corroborated by the large volumes of accretion onshore of the initial placement in the elevation surveys. The general agreement between elevation surveys and CoastSat results highlight the value of this new, low-cost measurement technique. The errors associated with the CoastSat extracted shoreline are due to temporal and spatial differences in wave setup and runup across the study site and dataset. When comparing to the survey extracted shorelines, this error may be influenced by survey and interpolation errors, although for this analysis we considered these errors to be minimal. With these considerations, the shoreline errors ranged between 3.69 to 9.96 m, consistent with previous applications [60]. Additionally, CoastSat results over the past 20 years show that the area is generally erosive between beachfill projects, providing relevant context for the shoreline gain observed following the nearshore nourishment. The long satellite record could be used during future feasibility studies to quantify background, natural shoreline variability in the system.

Observations suggest that the nearshore nourishment at Harvey Cedars had a positive impact on the adjacent beach, addressing a number of the factors that motivated beneficial use of dredged sediment at this location. This project provides the opportunity to assess the rapid modeling techniques that are used for nearshore nourishment siting. Volume change and centroid calculations from elevation surveys corroborate the Sediment Mobility Tool prediction that the placement would be very active. Nearshore berm deflation predictions following Bain et al. [54] are intended to provide order of magnitude estimates with a target of less than 200% error. This target is met for bulk removal rate predictions, with an error of 145%. Additionally, the fraction of predicted transport following Bain et al. [54] that is directed onshore (48%) is very similar to the measured ratio of onshore accretion to nearshore berm deflation (59%).

A number of factors could contribute to the relatively large deflation over-predictions. The methodology of Bain et al. [54] does not modify the nearshore berm shape as it deflates or reduce the volume of sediment available for transport. Keeping the same crest elevation causes an increased deflation bias, and considering the placement as an infinite sediment source does not prevent the deflation prediction to exceed the measured placement volume. The prediction of approximately equal alongshore sediment transport to the north and

south is not supported by measured elevation data. This unrealistic prediction could be related to the simple shore-parallel contour assumption omitting bathymetry impacts that were important to wave transformation in this case. While these simplifications appear to impact prediction accuracy, bulk deflation rates have less than 200% error, and the ratio between predicted onshore and alongshore transport may be reasonable, which emphasizes the value of this rapid technique.

5. Conclusions

In the summer of 2021, the USACE Philadelphia District beneficially used material dredged from Barnegat Inlet in a 67,500 m³ nearshore nourishment at an erosional hotspot in Harvey Cedars, NJ, USA. This nearshore nourishment was extensively monitored to describe the morphology change of the placed feature and adjacent beach. Nine topographic and bathymetric surveys were conducted, covering pre-construction and the first 302 days following construction. Wave information was measured at 1.5 m, 8 m, and 15.2 m depths. These measurements indicate that the placement was active, and sediment was transported from the placement footprint. Elevation surveys show shoreline advance over much of the measured area, centroid movement onshore and generally to the north, and volume gain onshore and south of the initial placement footprint.

Between 25 August 2021 and 22 March 2022, elevation surveys indicate that the placement eroded by 40% of the original volume. The net sediment gain in the surveyed area is 39,000 m³, which is the deflation volume (26,700 m³) from the nourishment footprint subtracted from the volume gain in the surrounding area (65,700 m³). This indicates the sheltering capacity of the nourishment for 7 months captured 58% of the placed volume from the longshore transport.

This is the first nearshore nourishment project to be investigated with satellite imagery using CoastSat. When compared to observed shoreline change, satellite-derived shoreline errors range from 3.69 to 9.96 m, which is consistent with past work, and results match elevation survey observations of more accretion onshore of the placement and to the south. The high temporal frequencies and spatial coverage at which the CoastSat analysis can be conducted, and the low cost make this a useful addition to capture shoreline change between elevation surveys. It could allow for new capabilities at locations that have not historically been able to monitor nearshore nourishments extensively.

Observed elevation changes also generally match predictions from the rapid assessment tools. Frequency of sediment mobilization and depth of closure estimates from the Sediment Mobility Tool both suggest that the placement should be active. The deflation predictions following Bain et al. [54] also imply that the placement should be active, but the predicted bulk deflation rates exceeded measured values by 145%. Agreement between predicted and observed behavior demonstrate the utility of these rapid tools while planning and designing nearshore nourishments.

Measured data, CoastSat analysis, and rapid predictions all indicate that the nearshore nourishment at Harvey Cedars had a positive impact on the adjacent beach. Data collected can be used to improve numerical modeling capabilities of nearshore nourishments. Future work can quantify long-term benefits of the nearshore nourishment, including the financial savings to the subaerial CSR project by beneficially placing dredged sediment in the nearshore.

Author Contributions: Conceptualization, M.A.C., B.C.M. and D.R.K.; methodology, B.C.M., B.D.H., D.R.K., S.P.M. and R.L.B.; software, R.L.B., S.P.M., N.R.O. and B.C.M.; formal analysis, B.C.M., D.R.K., R.L.B. and S.P.M.; investigation, B.C.M., B.D.H., D.R.K. and S.P.M.; writing—original draft preparation, S.P.M., D.R.K., B.C.M. and B.D.H.; writing—review and editing, S.P.M., B.D.H., B.C.M., D.R.K., R.L.B., N.R.O., I.W.C. and M.A.C.; visualization, R.L.B., S.P.M., N.R.O., B.C.M. and B.D.H.; project administration, S.P.M., B.D.H., B.C.M. and D.R.K.; funding acquisition, M.A.C., B.C.M., D.R.K. and B.D.H. All authors have read and agreed to the published version of the manuscript.

Funding: This research was funded by the U.S. Army Corps of Engineers through the Regional Sediment Management (RSM) Program, Coastal Inlets Research Program (CIRP), and the Water Resource and Development Act (WRDA) Section 1122 program.

Institutional Review Board Statement: Not applicable.

Data Availability Statement: The data presented in this study are available on request from the corresponding author.

Acknowledgments: We would like to thank the Borough of Harvey Cedars and the NJ Department of Environmental Protection's Office of Coastal Engineering for their support and assistance with this project. We would like to thank the USACE Philadelphia District for assistance with surveying, historical data, and instrument deployment/recovery.

Conflicts of Interest: The authors declare no conflict of interest.

References

- Zwamborn, J.A.; Fromme, G.A.W.; Fitzpatrick, J.B. Underwater mound for the protection of Durban's beaches. In Proceedings of the 12th International Conference on Coastal Engineering, Washington, DC, USA, 13–18 September 1970.
- Vera-Cruz, D. Artificial nourishment of Copacabana beach. In Proceedings of the 13th International Conference on Coastal Engineering, Vancouver, BC, Canada, 10–14 July 1972.
- Hanson, H.; Brampton, A.; Capobianco, M.; Dette, H.H.; Hamm, L.; Laustrup, C.; Lechuga, A.; Spanhoff, R. Beach nourishment projects, practices, and objectives—A European overview. *Coast. Eng.* **2002**, *47*, 81–111. [CrossRef]
- Lodder, Q.J.; Sørensen, P. Comparing the Morphological Behaviour of Dutch–Danish Shoreface Nourishments. In Proceedings of the Coastal Management: Changing Coast, Changing Climate, Changing Minds, Amsterdam, The Netherlands, 8–9 September 2015.
- Pinto, C.A.; Taborda, R.; Andrade, C.; Baptista, P.; Silva, P.A.; Mendes, D.; Pais-Barbosa, J. Morphological Development and Behaviour of a Shoreface Nourishment in the Portuguese Western Coast. *J. Mar. Sci. Eng.* **2022**, *10*, 146. [CrossRef]
- Mendes, D.; Pais-Barbosa, J.; Baptista, P.; Silva, P.A.; Bernardes, C.; Pinto, C. Beach Response to a Shoreface Nourishment (Aveiro, Portugal). *J. Mar. Sci. Eng.* **2021**, *9*, 1112. [CrossRef]
- Walker, B.M.; Krafft, D.R.; McFall, B.C.; McCaw, H.; Spurgeon, S.L. *Current State of Practice of Nearshore Nourishment by the United States Army Corps of Engineers*; ERDC/CHL SR-22-4; U.S. Army Corps of Engineers Engineer Research and Development Center: Vicksburg, MS, USA, 2022; 49p. [CrossRef]
- Brand, E.; Ramaekers, G.; Lodder, Q. Dutch experience with sand nourishments for dynamic coastline conservation—An operational overview. *Ocean Coast. Manag.* **2022**, *217*, 106008. [CrossRef]
- McFall, B.C.; Krafft, D.R.; McCaw, H.; Walker, B.M. *Metrics of Success for Nearshore Nourishment Projects Constructed with Dredged Sediment*; ERDC/TN RSM-21-3; U.S. Army Corps of Engineers Engineer Research and Development Center: Vicksburg, MS, USA, 2021; 13p. [CrossRef]
- Wang, P.; Brutsché, K.E.; Beck, T.M.; Rosati, J.D.; Lillycrop, L.S. *Initial Morphologic Evolution of Perdido Key Berm Nourishment, Florida*; ERDC/CHL CHETN-IV-89; U.S. Army Corps of Engineers Engineer Research and Development Center: Vicksburg, MS, USA, 2013; 10p, Available online: <http://hdl.handle.net/11681/2001> (accessed on 7 October 2022).
- Brutsché, K.E.; Wang, P.; Beck, T.M.; Rosati, J.D.; Legault, K.R. Morphological evolution of a submerged artificial nearshore berm along a low-wave microtidal coast, Fort Myers Beach, west central Florida, USA. *Coast. Eng.* **2014**, *91*, 29–44. [CrossRef]
- Brutsché, K.E.; McFall, B.C.; Li, H.; McNinch, J.E.; Ousley, J.D.; Engle, J.A.; Maglio, C.K. Strategic nearshore placement of dredged sediment at Vilano Beach, Florida. *Shore Beach* **2017**, *85*, 77–84.
- Otay, E.N. Monitoring results of a nearshore disposal berm. In Proceedings of the Coastal Dynamics '95, Gdańsk, Poland, 4–8 September 1995.
- Armstrong, S.B.; Lazarus, E.D.; Limber, P.W.; Goldstein, E.B.; Thorpe, C.; Ballinger, R.C. Indications of a Positive Feedback between Coastal Development and Beach Nourishment: Coastal Development Beach Nourishment. *Earth's Future* **2016**, *4*, 626–635. [CrossRef]
- McFall, B.C.; Brutsché, K.E.; Ousley, J.D.; Maglio, C.K.; Engle, J.A. Innovative nearshore berm placement techniques at Vilano Beach, FL, and application of the sediment mobility tool. *World Dredg.* **2017**, *51*, 34–35.
- Krafft, D.R.; Young, D.L.; Brutsché, K.E.; McFall, B.C.; Bruder, B.L. *Nearshore Placement Workshop 2019: Sediment Nourishment of the Nearshore Environment*; ERDC/CHL SR-20-02; U.S. Army Corps of Engineers Engineer Research and Development Center: Vicksburg, MS, USA, 2020; 28p. [CrossRef]
- van Duin, M.J.P.; Wiersma, N.R.; Walstra, D.J.R.; Van Rijn, L.C.; Stive, M.J.F. Nourishing the shoreface: Observations and hindcasting of the Egmond case, The Netherlands. *Coast. Eng.* **2004**, *51*, 813–837. [CrossRef]
- Hamilton, D.G.; Ebersole, B.A.; Smith, E.R.; Wang, P. *Development of a Large-Scale Laboratory Facility for Sediment Transport Study*; ERDC/CHL TR-01-22; U.S. Army Corps of Engineers Engineer Research and Development Center: Vicksburg, MS, USA, 2001; 187p. Available online: <http://hdl.handle.net/11681/7560> (accessed on 7 October 2022).

19. Smith, E.R.; Mohr, M.C.; Chader, S.A. Laboratory experiments on beach change due to nearshore mound placement. *Coast. Eng.* **2017**, *121*, 119–128. [[CrossRef](#)]
20. Hands, E.B.; Allison, M.C. Mound migration in deeper water and methods of categorizing active and stable depths. In Proceedings of the Coastal Sediments '91, Seattle, WA, USA, 25–27 June 1991.
21. Ahrens, J.P.; Hands, E.B. Parameterizing Beach Erosion/Accretion Conditions. In Proceedings of the Coastal Engineering 1998, Copenhagen, Denmark, 22–26 June 1998. [[CrossRef](#)]
22. Huisman, B.J.A.; Walstra, D.-J.R.; Radermacher, M.; de Schipper, M.A.; Ruessink, B.G. Observations and Modelling of Shoreface Nourishment Behaviour. *J. Mar. Sci. Eng.* **2019**, *7*, 59. [[CrossRef](#)]
23. Priestas, A.M.; McFall, B.C.; Brutsché, K.E. *Performance of Nearshore Berms from Dredged Sediments: Validation of the Sediment Mobility Tool*; ERDC/CHL TR-19-19; U.S. Army Corps of Engineers Engineer Research and Development Center: Vicksburg, MS, USA, 2019; 63p. [[CrossRef](#)]
24. McFall, B.C.; Brutsché, K.E.; Priestas, A.M.; Krafft, D.R. Evaluation Techniques for the Beneficial Use of Dredged Sediment Placed in the Nearshore. *J. Waterw. Port Coast. Ocean Eng.* **2021**, *147*, 04021016. [[CrossRef](#)]
25. Douglass, S.L. Estimating landward migration of nearshore constructed sand mounds. *J. Waterw. Port Coast. Ocean Eng.* **1995**, *121*, 247–250. [[CrossRef](#)]
26. Larson, M.; Ebersole, B.A. *An Analytical Model to Predict the Response of Mounds Placed in the Offshore*; ERDC/CHL CETN-II-42; U.S. Army Corps of Engineers Engineer Research and Development Center: Vicksburg, MS, USA, 1999; 13p. Available online: <http://hdl.handle.net/11681/2124> (accessed on 7 October 2022).
27. Johnson, C.L.; McFall, B.C.; Krafft, D.R.; Brown, M.E. Sediment Transport and Morphological Response to Nearshore Nourishment Projects on Wave-Dominated Coasts. *J. Mar. Sci. Eng.* **2021**, *9*, 1182. [[CrossRef](#)]
28. Smith, E.R.; D'Alessandro, F.; Tomasicchio, G.R.; Gailani, J.Z. Nearshore placement of a sand dredged mound. *Coast. Eng.* **2017**, *126*, 1–10. [[CrossRef](#)]
29. Bryant, D.B.; McFall, B.C. Transport of nearshore dredge material berms. In Proceedings of the 6th International Conference on Application of Physical Modelling in Coastal and Port Engineering and Science, Ottawa, ON, Canada, 10–13 May 2016.
30. de Schipper, M.A.; de Vries, S.; Ranasinghe, R.; Reniers, A.J.H.M.; Stive, M.J.F. Morphological developments after a beach and shoreface nourishment at Vlugtenburg beach. In Proceedings of the NCK-days 2012: Crossing borders in coastal research, Enschede, The Netherlands, 13–16 March 2012.
31. Gijman, R.; Visscher, J.; Schlurmann, T. A method to systematically classify design characteristics of sand nourishments. In Proceedings of the 36th International Conference on Coastal Engineering, Baltimore, MD, USA, 30 July–3 August 2018. [[CrossRef](#)]
32. Young, D.L.; Brutsché, K.E.; Li, H.; McFall, B.C.; Maloney, E.C.; McClain, K.E.; Bucaro, D.F.; LeRoy, J.Z.; Duncker, J.J.; Johnson, K.K.; et al. *Analysis of Nearshore Placement of Sediments at Ogden Dunes, Indiana*; ERDC/CHL TR-20-4; U.S. Army Corps of Engineers Engineer Research and Development Center: Vicksburg, MS, USA, 2020; 98p. [[CrossRef](#)]
33. de Looft, H.; Welp, T.; Snider, N.; Wilmink, R. Chapter 7: Adaptive Management. In *International Guidelines on Natural and Nature-Based Features for Flood Risk Management*; Bridges, T.S., King, J.K., Simm, J.D., Beck, Collins, G., Lodder, Q., Mohan, R.K., Eds.; U.S. Army Corps of Engineers Engineer Research and Development Center: Vicksburg, MS, USA, 2021.
34. Lodder, Q.; Jeuken, C.; Reinen-Hamill, R.; Burns, O.; Ramsdell, R., III; de Vries, J.; McFall, B.; Ijff, S.; Maglio, C.; Wilmink, R. Chapter 9: Beaches and Dunes. In *International Guidelines on Natural and Nature-Based Features for Flood Risk Management*; Bridges, T.S., King, J.K., Simm, J.D., Beck, Collins, G., Lodder, Q., Mohan, R.K., Eds.; U.S. Army Corps of Engineers Engineer Research and Development Center: Vicksburg, MS, USA, 2021.
35. Tyler, Z.J.; McFall, B.C.; Brutsché, K.E.; Maloney, E.C.; Bucaro, D.F. *Physical Monitoring Methods for the Nearshore Placement of Dredged Sediment*; ERDC/TN RSM-18-6; U.S. Army Corps of Engineers Engineer Research and Development Center: Vicksburg, MS, USA, 2018; 13p. [[CrossRef](#)]
36. van Rees, C.B.; Naslund, L.; Hernandez-Abrams, D.D.; McKay, S.K.; Woodson, C.B.; Rosemond, A.; McFall, B.; Altman, S.; Wenger, S.J. A strategic monitoring approach for learning to improve natural infrastructure. *Sci. Total Environ.* **2022**, *832*, 155078. [[CrossRef](#)]
37. Arnold, D.E.; McFall, B.C.; Brutsché, K.E.; Maloney, E.C.; Bucaro, D.F. *Nearshore Placement Techniques in Southern Lake Michigan*; ERDC/CHL TR-18-3; U.S. Army Corps of Engineers Engineer Research and development Center: Vicksburg, MS, USA, 2018; 45p. [[CrossRef](#)]
38. USACE Philadelphia District. *WRDA 2016 Section 1122 Beneficial Use of Dredged Material Pilot Program: Beneficial Use Placement Opportunities in New Jersey Using Navigation Channel Sediments—Barnegat Inlet*. 2021. Available online: https://www.nap.usace.army.mil/Portals/39/docs/Civil/Coastal/Barnegat-Inlet-Section-1122-April-2021.pdf?ver=mDQWxLcR_kkLqf_2ndOvIg%3D%3D (accessed on 7 October 2022).
39. Harris, B.D.; McGill, S.P.; Krafft, D.R.; McFall, B.C.; Chasten, M.A.; Bain, R.L. Beneficial Use of Dredged Material for Beach Erosion Mitigation at Harvey Cedars, New Jersey. *World Dredg.* **2022**, *55*, 10–11.
40. Vos, K.; Splinter, K.D.; Harley, M.D.; Simmons, J.A.; Turner, I.L. CoastSat: A Google Earth Engine-enabled Python toolkit to extract shorelines from publicly available satellite imagery. *Environ. Model. Softw.* **2019**, *122*, 104528. [[CrossRef](#)]
41. Cialone, M.A.; Thompson, E.F. *Wave Climate and Littoral Sediment Transport Potential, Long Beach Island, New Jersey*; ERDC/CHL TR-00-21; U.S. Army Corps of Engineers Engineer Research and Development Center: Vicksburg, MS, USA, 2000; 75p. Available online: <http://hdl.handle.net/11681/7451> (accessed on 7 October 2022).

42. Dally, W.R.; Osiecki, D.A. Evaluating the Impact of Beach Nourishment on Surfing: Surf City, Long Beach Island, New Jersey, U.S.A. *J. Coast. Res.* **2018**, *34*, 793–805. [[CrossRef](#)]
43. Hallermeier, R.J. Uses for a calculated limit depth to beach erosion. In Proceedings of the 16th International Conference on Coastal Engineering, Hamburg, Germany, 27 August–3 September 1978; pp. 1493–1512.
44. Hallermeier, R.J. A profile zonation for seasonal sand beaches from wave climate. *Coast. Eng.* **1981**, *4*, 253–277. [[CrossRef](#)]
45. Birkemeier, W.A. Field data on seaward limit of profile change. *J. Waterw. Port Coast. Ocean Eng.* **1985**, *111*, 598–602. [[CrossRef](#)]
46. Brutsché, K.E.; Rosati III, J.; Pollock, C.E.; McFall, B.C. *Calculating Depth of Closure Using WIS Hindcast Data*; ERDC/CHL CHETN-VI-45; U.S. Army Corps of Engineers Engineer Research and Development Center: Vicksburg, MS, USA, 2016; 9p. Available online: <http://hdl.handle.net/11681/20259> (accessed on 7 October 2022).
47. McFall, B.C.; Smith, S.J.; Pollock, C.E.; Rosati, J.; Brutsché, K.E. *Evaluating Sediment Mobility for Sitting Nearshore Berms*; ERDC/CHL CHETN-IV-108; U.S. Army Corps of Engineers Engineer Research and Development Center: Vicksburg, MS, USA, 2016; 11p. Available online: <http://hdl.handle.net/11681/20282> (accessed on 7 October 2022).
48. Larson, M.; Kraus, N.C. *Analysis of Cross-Shore Movement of Natural Longshore Bars and Material Placed to Create Longshore Bars*; Technical Rep. No. DRP-92-5; Department of the Army, Waterways Experiment Station, Corps of Engineers: Vicksburg, MS, USA, 1992; 124p. Available online: <http://hdl.handle.net/11681/4617> (accessed on 7 October 2022).
49. McFall, B.C.; Brutsché, K.E. *User's Guide for the Sediment Mobility Tool Web Application*; ERDC/TN RSM-18-4; U.S. Army Corps of Engineers Engineer Research and Development Center: Vicksburg, MS, USA, 2018; 11p. [[CrossRef](#)]
50. Komar, P.D. *Beach Processes and Sedimentation*, 2nd ed; Prentice Hall: Upper Saddle River, NJ, USA, 1998.
51. Dean, R.G.; Dalrymple, R.A. *Coastal Processes with Engineering Applications*; Cambridge University Press: Cambridge, UK, 2002.
52. Dean, R.G. *Beach Nourishment: Theory and Practice*; Advanced Series on Ocean Engineering, vol. 18; World Scientific Publishing Company Inc.: Hackensack, NJ, USA, 2002.
53. Soulsby, R.L. *Dynamics of Marine Sands*; Thomas Telford Publications: London, UK, 1997.
54. Bain, R.; McFall, B.; Krafft, D.; Hudson, A. Evaluating Transport Formulations for Application to Nearshore Berms. *J. Waterw. Port Coast. Ocean Eng.* **2021**, *147*, 4021031. [[CrossRef](#)]
55. Shaeri, S.; Etemad-Shahidi, A.; Tomlinson, R. Revisiting Longshore Sediment Transport Formulas. *J. Waterw. Port Coast. Ocean Eng.* **2020**, *146*, 4020009. [[CrossRef](#)]
56. Dronkers, J. *Dynamics of Coastal Systems*, 2nd ed.; World Scientific Publishing: Hackensack, NJ, USA, 2016.
57. Hudson, A.; Moritz, H.R.; Norton, J. *Sediment Mobility, Closure Depth, and the Littoral System—Oregon and Washington Coast*; ERDC/TN RSM-22-7; U.S. Army Corps of Engineers Engineer Research and Development Center: Vicksburg, MS, USA, 2022; 10p. [[CrossRef](#)]
58. Otsu, N. A Threshold Selection Method from Gray-Level Histograms. *IEEE Trans. Syst. Man Cybern.* **1979**, *9*, 62–66. [[CrossRef](#)]
59. Grunnet, N.M.; Ruessink, B.G. Morphodynamic response of nearshore bars to a shoreface nourishment. *Coast. Eng.* **2005**, *52*, 119–137. [[CrossRef](#)]
60. Vos, K.; Harley, M.D.; Splinter, K.D.; Simmons, J.A.; Turner, I.L. Sub-annual to multi-decadal shoreline variability from publicly available satellite imagery. *Coast. Eng.* **2019**, *150*, 160–174. [[CrossRef](#)]